A&A 452, 285–294 (2006)
DOI: 10.1051/0004-6361:20054077

Astronomy & Astrophysics

INTEGRAL and *RXTE* monitoring of GRS 1758−258 in 2003 and 2004

A transition from the dim soft state to the hard state

K. Pottschmidt[1], M. Chernyakova[2,⋆], A. A. Zdziarski[3], P. Lubiński[3,2], D. M. Smith[4], and N. Bezayiff[4]

[1] Center for Astrophysics and Space Sciences, University of California, San Diego, La Jolla, CA 92093-0424, USA
e-mail: kpottschmidt@ucsd.edu
[2] *INTEGRAL* Science Data Centre, Chemin d'Écogia 16, 1290 Versoix, Switzerland
[3] Nicolaus Copernicus Astronomical Center, Bartycka 18, 00-716 Warszawa, Poland
[4] Department of Physics, University of California, Santa Cruz, Santa Cruz, CA 95064, USA

Received 20 August 2005 / Accepted 4 February 2006

ABSTRACT

The Galactic Center black hole candidate (BHC) GRS 1758−258 has been observed extensively within *INTEGRAL*'s Galactic Center Deep Exposure (GCDE) program in 2003 and 2004, while also being monitored with *RXTE*. We present quasi-simultaneous PCA, ISGRI, and SPI spectra from four GCDE observation epochs as well as the evolution of energy-resolved PCA and ISGRI light curves on time scales of days to months. We find that during the first epoch GRS 1758−258 displayed another of its peculiar dim soft states like the one observed in 2001, increasing the number of observed occurrences of this state to three. During the other epochs the source was in the hard state. The hard X-ray emission component in the epoch-summed spectra can be well described either by phenomenological models, namely a cutoff power law in the hard state and a pure power law in the dim soft state, or by thermal Comptonization models. A soft thermal component is clearly present in the dim soft state and might also contribute to the softer hard state spectra. We argue that in the recently emerging picture of the hardness-intensity evolution of black hole transient outbursts in which hard and soft states are observed to occur in a large overlapping range of luminosities (hysteresis), the dim soft state is not peculiar. As noted before for the 2001 dim soft state, these episodes seem to be triggered by a sudden decrease (within days) of the hard emission, with the soft spectral component decaying on a longer time scale (weeks). We discuss this behavior as well as additional flux changes observed in the light curves in terms of the existence of two accretion flows characterized by different accretion time scales, the model previously suggested for the 2001 episode.

Key words. black hole physics – stars: individual: GRS 1758−258 – gamma rays: observations – X-rays: binaries – X-rays: general

1. Introduction

The hard X-ray source GRS 1758−258 was discovered in 1990 (Mandrou 1990; Sunyaev et al. 1991) during observations of the Galactic Center region performed with the *Granat* satellite. Most of the time the source displays X-ray properties similar to the canonical hard state of Galactic black hole binaries, i.e., a comparatively hard spectrum with power law indices of $\Gamma = 1.4-1.9$ and an exponential cutoff above 100 keV (Kuznetsov et al. 1999; Main et al. 1999; Lin et al. 2000) as well as strong short term variability on frequencies up to 10 Hz which can be characterized by a flat-topped power spectrum (Smith et al. 1997; Lin et al. 2000). Based on these X-ray properties and on the detection of a radio counterpart (a point source plus a double-sided jet structure, Rodriguez et al. 1992) GRS 1758−258 is considered to be a microquasar.

With the exception of rare dim soft states that can last up to several months, the X-ray emission of GRS 1758−258 is persistent. In contrast to the canonical picture for persistent black hole binaries, however, GRS 1758−258 most likely has a low mass binary companion and is accreting via Roche lobe overflow. Three faint IR counterpart candidates have been identified recently, multi-band photometry and near-infrared spectroscopy characterizing the brightest of them as a probable K0 III giant and the other two as main sequence A stars (Marti et al. 1998; Goldwurm et al. 2001; Eikenberry et al. 2001; Rothstein et al. 2002; Heindl & Smith 2002a). Taking into account the 18.45 ± 0.10 day binary orbit (Smith et al. 2002a), the radius of a K giant is consistent with Roche lobe overflow, while the other counterpart candidates are too small (Rothstein et al. 2002).

From 1990 to 1998 the source was monitored in the hard X-ray regime with *Granat*/SIGMA, establishing it as persistent hard state black hole binary but also revealing a factor of eight variability in the 40−150 keV flux (Kuznetsov et al. 1999). At softer X-rays monitoring of GRS 1758−258 (and its "sister source" 1E 1740.7−2942) with *RXTE* started with monthly observations in 1996 and is still on-going in 2005, with two observations each week (Main et al. 1999; Smith et al. 1997, 2001a, 2002a,b, this work). This campaign led to the discovery that in GRS 1758−258 (and 1E 1740.7−2942) the observed spectral hardness is not anti-correlated with the 2−25 keV flux but rather correlated with the flux derivative – in the sense that the spectrum is softest when the 2−25 keV count rate is dropping. This behavior is different from the prototype hard state black hole binary Cyg X-1 which is showing the canonical anti-correlation of spectral hardness and soft X-ray flux. It has been interpreted as an indication for the presence of two *independent*

⋆ On leave from the Astro Space Center of the P.N. Lebedev Physical Institute, 84/32 Profsoyuznaya Street, Moscow 117997, Russia.

accretion flows supplied with proportional amounts of matter at large radii which are then accreted on different time scales (Main et al. 1999; Smith et al. 2002b): a hot, e.g., ADAF-type, accretion flow, reacting quickly to changes in the accretion rate, and a large accretion disk with a long viscous time scale (consistent with accretion via Roche lobe overflow). In addition, Lin et al. (2000) performed a radio to γ-ray multi-wavelength study of the hard state as observed in 1997 August, including spectral modeling and high time resolution analyses. Applying the thermal Comptonization model `compTT` (Titarchuk 1994) they obtained a temperature of 52 keV and an optical depth of 3.4 for the hot plasma. Sidoli & Mereghetti (2002) obtained very similar values using `compTT` to model a broad band *BeppoSAX* spectrum of the source obtained in 1997 April.

A weak soft excess is sometimes seen in the hard state spectra of GRS 1758−258 (Heindl & Smith 1998; Lin et al. 2000) or cannot be excluded to be present (Mereghetti et al. 1997). It has also been observed in conjunction with a slightly reduced hard X-ray flux during an intermediate state in 1993 March/April (Mereghetti et al. 1994). A similar recent episode in 2000 September has been characterized as an intermediate state based on the *RXTE* monitoring observations (Heindl & Smith 2002a, and references therein). Modeling an *XMM-Newton*/EPIC-MOS spectrum obtained during this time, Goldwurm et al. (2001) found that in addition to a comparatively soft power law ($\Gamma \sim 2$) a blackbody component ($kT_{\rm in} \sim 320$ eV) is required.

On two occasions a much softer and dimmer state than the persistent hard state with occasional softening has been observed: (i) A sudden drop of the 2−25 keV rate between one *RXTE* monitoring observation and the next occurred in 2001 February, with an estimated *decrease* of ∼35% of the 1.3−200 keV luminosity within ∼20 d after the transition (Smith et al. 2001a). An extreme case of the unusual flux derivative/hardness relation described above, this behavior is different from the canonical black hole state behavior where the soft state corresponds to a higher accretion rate and a higher bolometric luminosity. For the 1996 soft state of Cyg X-1, e.g., Zdziarski et al. (2002) find a 3−4 times higher bolometric luminosity than for the typical hard state, an increase even higher than the ∼50−70% estimated previously (Zhang et al. 1997). In Sect. 4 we suggest that the dim soft state can be better understood when compared to outbursts of BHC transients than to (focused) wind accretors like Cyg X-1. Smith et al. (2001a) also found that the transition to the 2001 dim soft state of GRS 1758−258 was mainly due to a decreasing and softening power law component ($\Gamma \sim 2.75$ in 2001 March), revealing a soft component ($kT_{\rm in} \sim 460$ eV in 2001 March). As predicted by Smith et al. (2001b) based on the two-flow accretion model, the soft component decayed more slowly than the hard one, on a time scale of ∼28 days. Displaying a complex structure, including a partial recovery of the count rates in 2001 July, the dim soft state lasted until 2001 December (Heindl & Smith 2002a, see also this work). *Chandra*/ACIS-HETGS (Heindl & Smith 2002a,b) and *XMM-Newton*/RGS (Miller et al. 2002) observations in 2001 March support the picture that the decaying soft flux is emitted by an accretion disk. (ii) It can be assumed that *Granat*/SIGMA exposures in fall 1991 and spring 1992 when the 40−150 keV flux was below the detection limit (Gilfanov et al. 1993) found the source in a similar dim soft state (Smith et al. 2001a; Miller et al. 2002). This is supported by the analysis of a 1992 March *ROSAT*/PSPC spectrum by Grebenev et al. (1997) resulting in a power law index of $\Gamma \sim 2.5$.

In the following we report results of monitoring observations of GRS 1758−258 with *INTEGRAL* and *RXTE* in 2003 and 2004. While the source was in its usual variable hard state during most of the time, the data obtained in spring 2003 clearly correspond to another dim soft state, although it did not progress as far as the 2001 dim soft state before the hard X-ray emission recovered again. In Sect. 2 of this paper we describe the observing strategy of the two monitoring programs and explain the data extractions performed to obtain broad band PCA-ISGRI-SPI spectra and multi-band PCA and ISGRI light curves. In Sect. 3.1 the long term light curves and flux changes are described and in Sect. 3.2 we present results of modeling the broad band spectra with phenomenological and thermal Comptonization models. The results, especially the observation of another weak soft state, are discussed in the light of current black hole outburst and accretion models in Sect. 4. Our conclusions are summarized in Sect. 5.

2. Observations and data reduction

During 2003 and 2004 the guaranteed time program amounted to 30−35% of *INTEGRAL*'s observing time and was mainly dedicated to the Galactic Plane Scan (GPS) and Galactic Center Deep Exposure (GCDE) projects within the *INTEGRAL* team's Core Programme. Especially the GCDE[1] provided a wealth of data on GRS 1758−258. All Core Programme data up to January 2005 as well as all data of the source public at that time have been included into the analysis presented here. Our *INTEGRAL* data are grouped into four data sets observed in spring and fall of 2003 and 2004 which in the following shall be called epoch 1−4. See Table 1 for more details.

We used version 4.2 of the Offline Scientific Analysis package for *INTEGRAL* to extract spectra and light curves of GRS 1758−258 obtained by the *INTEGRAL* Soft Gamma Ray Imager (ISGRI; Lebrun et al. 2003) detector as well as spectra from the SPectrometer on *INTEGRAL* (SPI; Vedrenne et al. 2003)[2]. See `http://integral.esac.esa.int/workshops/Jan2005/session1/lubinski_cross.pdf` for information on instrument cross-calibration issues for OSA 4.2. Due to the grid nature of the observations and the usually hard source spectrum, the smaller field of view Joint European X-ray Monitor (JEM-X; Lund et al. 2003) did not yield any useful data covering the epoch time scales. In order to extract the ISGRI data products, all pointings ("science windows", "ScWs") in which the offset of the source from the spacecraft pointing direction was smaller than 10° have been taken into account. For offsets in this range systematic effects in the Crab calibration spectra show the same general trends as for pointings in the fully coded field of view. This selection amounts to ∼1920 ScWs with an exposure of approximately 1800 s each. Average spectra for the four epochs were built by producing images in 12 energy bands for each ScW in a given epoch, extracting the GRS 1758−258 source flux from each image, and averaging the source fluxes of all ScWs in a given energy band using standard weighting techniques. This method is described in the ISGRI user manual (`http://isdc.unige.ch/doc/tec/um/user_support/ibis/ibis_4.2.pdf`) and is the

[1] Concentrating on 5° around the Galactic Center but with pointing positions reaching out to Galactic longitudes and latitudes of about ±30° and ±20°, respectively, from it.

[2] At the time of submission of this paper, OSA 5.0 had just become available. The conclusions presented in this work do not depend on the OSA version. Since OSA 4.2 extractions of ISGRI spectra for sources as faint as GRS 1758−258 require the use of the special procedure described in this section and since no experience with using OSA 5.0 for faint sources existed prior to submission, we decided to continue using OSA 4.2.

Table 1. *INTEGRAL* observing epochs for GRS 1758−258, giving the exposure times of the summed spectra analyzed for each epoch and instrument, including the *RXTE*/PCA.

Epoch[a]	Start & End Date	ISGRI [ks]	SPI [ks]	PCA[b,c] [ks]
1	2003/02/28−2003/04/23	511	–	27
2	2003/08/19−2003/10/14	1889	1358 1141[d]	19
3	2004/02/17−2004/04/20	578	759	23
4	2004/08/21−2004/10/28	467	615	10

[a] The four epochs correspond to *INTEGRAL* orbits 46−66, 103−122, 164−185, and 226−249.
[b] The PCA exposure includes only data from PCU 2, see text for more details.
[c] Data from the following *RXTE* programs are included: 50107, 80102, and 90102.
[d] SPI spectra for two non-overlapping data sets within this epoch have been extracted (orbits 103−111 and 112−122), see text for more details.

recommended procedure for all but the brightest sources. For the coded aperture instrument ISGRI the diffuse Galactic background is part of the background removed when reconstructing the sky images out of detector shadowgrams (Goldwurm et al. 2003; Terrier et al. 2003). For the spectral modeling we use the ancillary response file "isgr_arf_rsp_0006.fits" and a rebinned version of the response matrix "isgr_rmf_grp_0012.fits" distributed with OSA 4.2. In addition, light curves with a time resolution of 1000 s were produced in three energy bands: 20−60, 60−100, and 100−200 keV.

During the first epoch the source was too soft to be detected by the SPI instrument. For the remaining three epochs the same ScWs as for ISGRI were used to produce epoch-summed SPI spectra, with the exception of epoch 2, where successful OSA runs could only be obtained by splitting the SPI data into two subsets. The difference in the exposure times given for ISGRI and SPI in Table 1 are mainly due to ISGRI's dead-time. The SPI spectra were extracted over an energy range of 20−500 keV (25 bins) using the SPIROS package within OSA, applying maximum likelihood optimization statistics (Skinner & Connell 2003). We set the number of pseudo detectors to 84 (i.e., including events located near borders between the physical SPI detectors and registered in more than one of them) and selected background correction method 5 (detector averaged count rate modulation model). The input catalog of sources consisted of the 18 sources seen in the ISGRI 20−60 keV mosaic images. Alternative parameter settings were tested, like changing the number of pseudo detectors to 18 (i.e., including only single events), using background model 2 (each detector scaled separately), or allowing sources to be variable (SEL_FLAG = 2). None of these alternatives lead to a significant change in the obtained count rates. Applying an alternative extraction method optimized for recovering spatially extended emission, Strong et al. (2003) find that the diffuse Galactic background spectrum is of roughly power law shape, falling with a slope of 2.5−3. We verified that adding such a component to only the SPI data does not change the best fit parameters of the multi-instrument fits discussed in Sect. 3.2 and that the normalization of the new power law is consistent with zero. Note that according to a study by Dubath et al. (2005) based on observations and simulations, SPI fluxes of sources *with known positions* can be well recovered down to a source separation of at least 0.°5. With an angular distance of 0.°66 from GRS 1758−258 the nearest source, the bright LMXB GX 5−1, should therefore not contaminate our GRS 1758−258 SPI spectra. For the data sets presented here a careful inspection of the spectra of both sources shows no indication of contamination with the possible exception of one bin affected by an overcorrection (undercorrection) of the 66.7 keV background line for GRS 1758−258 (GX 5−1). We find, however, that excluding this bin from the analysis does not change the results.

In order to characterize the source behavior at softer X-ray energies we use data from *RXTE*'s Proportional Counter Array (PCA; Jahoda et al. 1996) obtained during the on-going *RXTE* monitoring campaign. Under this program 1.5 ks snapshots of GRS 1758−258 have been taken monthly in 1996, weekly from 1997 through 2000, and approximately twice each week since then. For a description of the offset observing strategy applied to avoid nearby sources and of the extra background measurements taken to minimize the influence of the diffuse Galactic emission see Smith et al. (1997) and Main et al. (1999). This procedure has been successfully evaluated using data from the pronounced dim soft state in 2001. Reduction of the PCA data was performed using the HEASOFT package version 5.3.1. The responses were generated using pcarsp version 10.1 (see `http://lheawww.gsfc.nasa.gov/docs/xray/xte/pca/` for more information on the *RXTE*/PCA energy calibration under this HEASOFT version). Average spectra for the four *INTEGRAL* observing epochs were produced. In addition, long term light curves consisting of the average count rates of each PCA monitoring pointing were generated in three energy bands (2.5−4, 4−10, and 10−25 keV) and for the overall 2.5−25 keV light curve. We only use data from PCA's top layer to optimize the signal to noise ratio. For the average spectra we additionally decided to select data from one of PCA's five Proportional Counter Units (PCUs), namely from PCU 2, only[3]. The loss of additional PCA exposure is acceptable since our aim is to study the broad band spectral continuum (and not, e.g., to perform deeper iron line studies) with emphasis on characterizing the hard spectral component, i.e., on the *INTEGRAL* data. This strategy also allows us to further minimize systematic effects due to PCU cross-calibration. See Table 1 for the total exposure times of the epoch-summed PCA spectra. Note that the All Sky Monitor (ASM) on *RXTE* is not well suited to observe GRS 1758−258: the source's daily 1.3−12.2 keV ASM rate averaged over the time of the *INTEGRAL* mission up 2005 March, e.g., is 2.0 ± 2.5 cps. Also, since the absorbed soft flux does not change much in the dim soft state (see next section), no change is seen in the ASM light curve around epoch 1.

3. Data analysis and results

3.1. Long term light curves and flux changes

Figure 1 shows the evolution of the *INTEGRAL* and *RXTE* light curves of GRS 1758−258 during the monitoring in 2003 and 2004 in several energy bands, spanning a total energy range of 2.5−200 keV. The *INTEGRAL* light curves have been rebinned to a resolution of one day, for *RXTE* the average count rate of each PCA data set is plotted, normalized to one PCU. The count rates during epoch 1 are significantly lower in all energy bands above 4 keV. Above 100 keV the source is not detected in epoch 1. The PCA measurements during and between epochs 1 and 2 suggest that the former almost exactly covers the last two months of a

[3] PCU 2 and PCU 3 are the units mainly used for monitoring. In the data sets discussed here PCU 1 and PCU 4 only contain ∼15−30% of the exposure of PCU 2 or PCU 3.

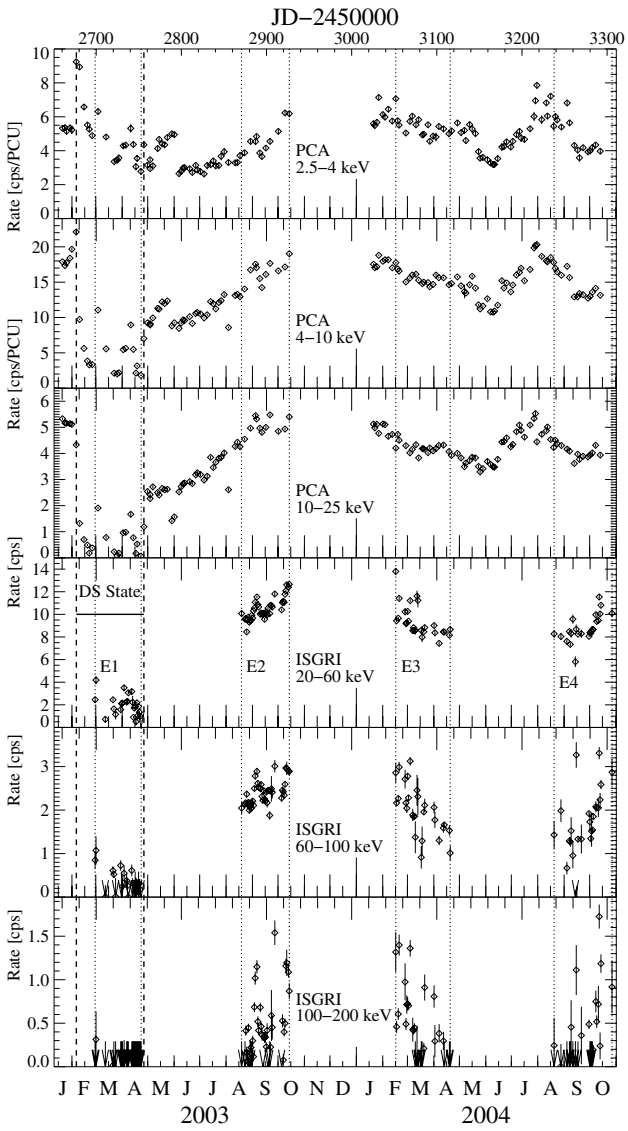

Fig. 1. *INTEGRAL*/ISGRI and *RXTE*/PCA light curves of GRS 1758−258 in the indicated energy ranges as observed in 2003 and 2004. The ISGRI light curves have been rebinned to a resolution of 1 d. Arrows indicate non-detections. For the PCA the average count rate of each monitoring observation is shown in all energy bands. Vertical dashed and dotted lines denote the dim soft state ("DS State") and the four *INTEGRAL* observation epochs ("E1"–"E4"), respectively.

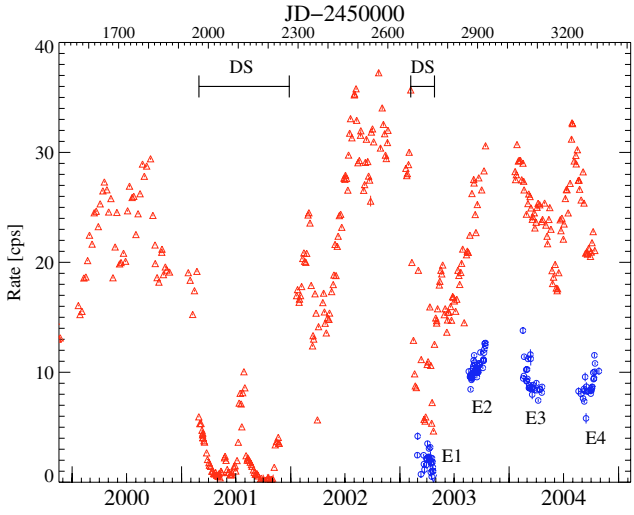

Fig. 2. Evolution of the 2.5−25 keV PCA count rates of GRS 1758−258 since 2000 (open triangles) and of the 20−60 keV ISGRI count rates in 2003/2004 (open circles, see also Fig. 1). The binning is the same as in Fig. 1. The dim soft states are denoted by "DS" and the four *INTEGRAL* observation epochs are again labeled "E1"–"E4".

Table 2. Average model flux for each epoch based on the best fit values of Table 3.

	Epoch 1	Epoch 2	Epoch 3	Epoch 4
$F^{b}_{2.5-4}$	1.6	1.4	1.4	1.5
F^{a}_{2-4}	4.2	2.3	2.5	2.8
$F^{a,c}_{3-9}$	1.9	4.7	4.5	4.7
F^{a}_{4-100}	2.5	22.9	18.7	18.6

[a] Unabsorbed flux in units of 10^{-10} erg cm^{-2} s^{-1}. The $N_{\rm H}$ values of Table 3 have been used for the flux correction.
[b] Absorbed flux in units of 10^{-10} erg cm^{-2} s^{-1}.
[c] See comparison with flux changes of GX 339−4 in Sect. 4.

~3 months long period during which the source was in a dim soft state and that a transition to the more common hard started with the end of epoch 1.

This picture is supported by the average flux values determined from our spectral fits (Table 2). The 4−100 keV flux is considerably reduced in epoch 1. Consistent with the light curves the *absorbed* 2.5−4 keV flux does not change much between the soft and hard state epochs. The *unabsorbed* flux extrapolated to slightly lower energies, namely 2−4 keV, reveals an overall brightening at very low energies in epoch 1, however. A similar behavior was also observed during the onset of the 2001 dim soft state (Smith et al. 2001a). Different from 2001, though, the 2003 dim soft state starts with a short peak in the soft 2.5−4 keV light curve, coinciding with the decay above 10 keV. The 4−10 keV light curve shows a superposition of both trends, with the flare dominating first and then the decay.

To put the *INTEGRAL* observing epochs into the broader context of the source history, Fig. 2 shows the 2.5−25 keV light curve from the PCA monitoring since 2000 as well as the 20−60 keV ISGRI light curve again. The dim soft state in 2001 is readily apparent, including two instances within the off phase (2001 May and 2001 July/August) where the source partly turns on again. The 2.5−4 keV and 10−25 keV overview light curves shown by Heindl & Smith (2002a) include these turn-ons. In their Fig. 1 it can be seen that the soft emission only reaches its minimum after the second turn-on. The soft emission decays slower than the hard emission after each turn-on, consistent with the two-flow scenario. The decrease of the 2.5−25 keV rate in 2003 February is slower than the rapid initial drop in 2001 February, but the 10−25 keV light curve in Fig. 1 reveals that the hard emission decreases on a similar time scale as in 2001, i.e., within about a week. The 2003 dim soft state is shorter and not declining below ~4 cps/PCU in the 2.5−25 keV band, though. In addition to the dim soft states there is considerable long term variability present in the light curves, the *INTEGRAL* 20−60 keV ISGRI rate, e.g., varies by a factor of 30−40% within each hard state epoch. Furthermore, the 2.5−25 keV PCA light curve shows several sudden count rate drops, less severe or shorter than the dim soft states, e.g., in 2002 March or between epochs 3 and 4 or during epoch 4.

Table 3. Best fit parameters for the power law models. The full model in XSPEC notation for epoch 1 is `const×phabs [diskbb+gauss+power]`, for epoch 2 it is `const×phabs[gauss+ cutoffpl]` and for epochs 3 and 4 `const×phabs[diskbb+gauss+ cutoffpl]`. Parameters shown are the hydrogen column density $N_{\rm H}$, the inner accretion disk temperature $kT_{\rm in}$ and its normalization $A_{\rm disk} = ((R_{\rm in}/{\rm km})/(D/10\,{\rm kpc}))^2 \cos i$, the power law index Γ and the power law cutoff energy $E_{\rm cutoff}$, the energy $E_{\rm Fe}$ and equivalent width $EW_{\rm Fe}$ of the Gaussian Fe Kα line, and the flux normalization constants of the individual instruments with respect to the PCA, $c_{\rm ISGRI}$ and $c_{\rm SPI}$.

	Epoch 1	Epoch 2	Epoch 3	Epoch 4
$N_{\rm H}/10^{22}$ [cm^{-2}]	$1.66^{+1.60}_{-0.41}$	$1.11^{+0.25}_{-0.20}$	1.50	$1.50^{+3.18}_{-1.20}$
$kT_{\rm in}$ [eV]	477^{+11}_{-27}	–	679^{+145}_{-66}	536^{+250}_{-222}
$A_{\rm disk}/10^3$	$2.7^{+0.9}_{-0.1}$	–	$0.04^{+0.05}_{-0.02}$	$0.16^{+0.41}_{-0.12}$
Γ	$2.29^{+0.10}_{-0.05}$	$1.54^{+0.01}_{-0.02}$	$1.59^{+0.03}_{-0.04}$	$1.69^{+0.05}_{-0.05}$
$E_{\rm cutoff}$ [keV]	–	185^{+22}_{-17}	136^{+13}_{-16}	246^{+26}_{-56}
$E_{\rm Fe}$ [keV]	$6.40^{+0.12}_{-0.19}$	$6.52^{+0.21}_{-0.27}$	$6.66^{+0.15}_{-0.24}$	$6.57^{+0.13}_{-0.37}$
$EW_{\rm Fe}$ [eV]	146.0	59.2	53.8	49.0
$c_{\rm ISGRI}$	$0.70^{+0.06}_{-0.06}$	$0.85^{+0.02}_{-0.02}$	$0.83^{+0.02}_{-0.03}$	$0.88^{+0.01}_{-0.02}$
$c_{\rm SPI}$	–	$0.99^{+0.02}_{-0.04}$	$1.00^{+0.05}_{-0.10}$	$1.00^{+0.11}_{-0.11}$
$\chi^2_{\rm noFe}$/d.o.f.	61.3/39	88.6/69	83.3/55	60.2/55
χ^2/d.o.f.	37.7/35	55.7/65	56.7/52	49.4/51
$\chi^2_{\rm red}$	1.08	0.86	1.09	0.97

Table 4. Best fit parameters for the `compTT` model. The full model in XSPEC notation is `const×phabs[diskbb+ gauss+compTT+reflect(compTT)]`, where for epoch 2 the `diskbb` component and for epochs 1 and 4 the `reflect(compTT)` component turned out not to be required. The parameters shown are mostly the same as in Table 3 but instead of the power law related parameters, the physical parameters associated with Comptonization and reflection are shown, namely the electron temperature of the Comptonizing plasma $kT_{\rm e}$ and its optical depth τ, and the covering factor of the cold reflecting medium $\Omega/2\pi$. $kT_{\rm in}$ in this table is either the temperature of the `diskbb` component and/or the seed photon input for the hot plasma.

	Epoch 1	Epoch 2	Epoch 3	Epoch 4
$N_{\rm H}/10^{22}$ [cm^{-2}]	$1.50^{+0.21}_{-0.26}$	$1.37^{+0.20}_{-0.15}$	1.50	1.50
$kT_{\rm in}$ [eV]	482^{+14}_{-16}	379^{+116}_{-378}	441^{+86}_{-55}	501^{+71}_{-90}
$A_{\rm disk}/10^3$	$2.5^{+0.4}_{-0.3}$	–	$0.38^{+0.54}_{-0.04}$	$0.28^{+0.72}_{-0.07}$
τ	$0.29^{+0.43}_{-0.13}$	$0.71^{+0.16}_{-0.07}$	$1.00^{+0.21}_{-0.21}$	$0.37^{+0.24}_{-0.12}$
$kT_{\rm e}$ [keV]	64^{+4}_{-15}	78^{+34}_{-15}	49^{+29}_{-9}	114^{+32}_{-35}
$E_{\rm Fe}$ [keV]	$6.41^{+0.13}_{-0.24}$	$6.62^{+0.21}_{-0.30}$	$6.74^{+0.15}_{-0.26}$	$6.47^{+0.32}_{-0.25}$
$EW_{\rm Fe}$ [eV]	208.0	61.0	42.6	64.3
$c_{\rm ISGRI}$	$0.76^{+0.08}_{-0.08}$	$0.83^{+0.03}_{-0.02}$	$0.82^{+0.01}_{-0.02}$	$0.87^{+0.02}_{-0.02}$
$c_{\rm SPI}$	–	$0.96^{+0.05}_{-0.04}$	$0.97^{+0.10}_{-0.09}$	$0.97^{+0.12}_{-0.11}$
$10^2\ \Omega/2\pi$	–	$10.0^{+5.6}_{-5.6}$	$13.8^{+5.0}_{-5.5}$	–
χ^2/d.o.f.	37.2/34	52.5/63	57.3/51	49.8/52
$\chi^2_{\rm red}$	1.09	0.83	1.12	0.96

3.2. Spectral analysis

3.2.1. Models and data preparation

Below 100 keV GRS 1758−258 has often been modeled by an absorbed power law (Sunyaev et al. 1991; Mereghetti et al. 1997; Main et al. 1999). Kuznetsov et al. (1999) found that an exponential cutoff power law fits the 1990−1997 *GRANAT* data above 100 keV better than a simple power law and Lin et al. (2000) obtained good fits to their joint *RXTE*/PCA, *RXTE*/HEXTE, and *CGRO*/OSSE spectrum of 1997 with a cutoff power law. Thermal Comptonization has also been shown to provide a good description of the hard state spectra (Kuznetsov et al. 1999; Lin et al. 2000; Keck et al. 2001). As reported in Sect. 1, an additional weak thermal component can be present in the hard state (Heindl & Smith 1998; Lin et al. 2000) which is more clearly revealed in the intermediate (Mereghetti et al. 1994; Goldwurm et al. 2001) and especially the dim soft state (Smith et al. 2001a; Miller et al. 2002; Heindl & Smith 2002a).

From initial power law fits to our *INTEGRAL* data alone, we found that for epochs 2 to 4 a cutoff is required. This is imposed by the ISGRI data sets. Due to SPI's comparatively small effective area, the SPI data do not carry enough weight to further constrain the cutoff energy. Our basic phenomenological model for the simultaneous fits to the summed *INTEGRAL*/*RXTE* spectra of each epoch thus consists of an absorbed cutoff power law plus a Gaussian Fe Kα line (see Sect. 3.2.2 for a discussion of the need to include the line), with an additional multicolor disk blackbody component if required. We also applied a thermal Comptonization model (`compTT`; Titarchuk 1994) to all four epochs, again including absorption, Fe emission, and the optional disk blackbody as well as allowing for a reflected Comptonized component (Magdziarz & Zdziarski 1995). Normalization differences between the instruments are taken into account in all fits by a multiplicative constant, set to 1 for the PCA. The exact model compositions of both, the phenomenological and the physical model, can be found in the captions of Tables 3 and 4 for all epochs.

We used XSPEC version 11.3.1t to perform the fits. Consistent with the recommendations of the calibration teams, systematic errors of 0.5% and 2% had to be added to all PCA and ISGRI spectra, respectively. PCA data from 3−20 keV, ISGRI data from 20−150 keV, and SPI data from 40−200 keV were taken into account in all fits, with the exception of epoch 1 where PCA data up to only 18 keV and ISGRI data up to only 100 keV were included. Both modeling approaches resulted in good descriptions of the data and produced similar $\chi^2_{\rm red}$ values for given epochs. Tables 3 and 4 list the best fit parameters and χ^2 values for the power law and the Comptonization models, respectively. Single parameter uncertainties are given on a 90% confidence level. The results quoted for epoch 2 contain both SPI data sets. Without the 2.5 Ms of SPI data, the $\chi^2_{\rm red}$ values of the epoch 2 fits are in better agreement with the quality of the other fits, e.g., $\chi^2_{\rm red} = 1.1$ for the epoch 2 `cutoffpl` fit (with no significant changes of the best fit parameters). Figures 3 and 4 show the counts spectra, best fit models, and residuals for the `compTT` fits.

Since the calibration of the *INTEGRAL* instruments, especially ISGRI, is work in progress, we expect that the best fit parameters characterizing the hard spectrum will be refined and updated in future iterations of this work. In this iteration we interpret them as indicators for general trends (e.g., the state change, qualitative consistency with canonical values, etc.). Modeling the spectra with Comptonization models also taking non-thermal electron distributions into account like `compPS` (Poutanen & Svensson 1996) or `eqpair` (Coppi 1999) will also be part of future work. However, consistency checks have been performed, applying the `compPS` model in a form comparable to our `compTT` fits (thermal electrons, slab geometry, optional multicolor disk blackbody). We obtain fits of similar quality, with seed photon temperatures, plasma temperatures and optical depths consistent with the `compTT` results. The reflection fraction obtained with `compPS` is systematically higher, though, e.g., 24% for epoch 2 compared to 10% with `compTT`. A similar trend of lower reflection fractions obtained with `compTT` was also observed between `eqpair` and `compTT` fits to Cyg X-1

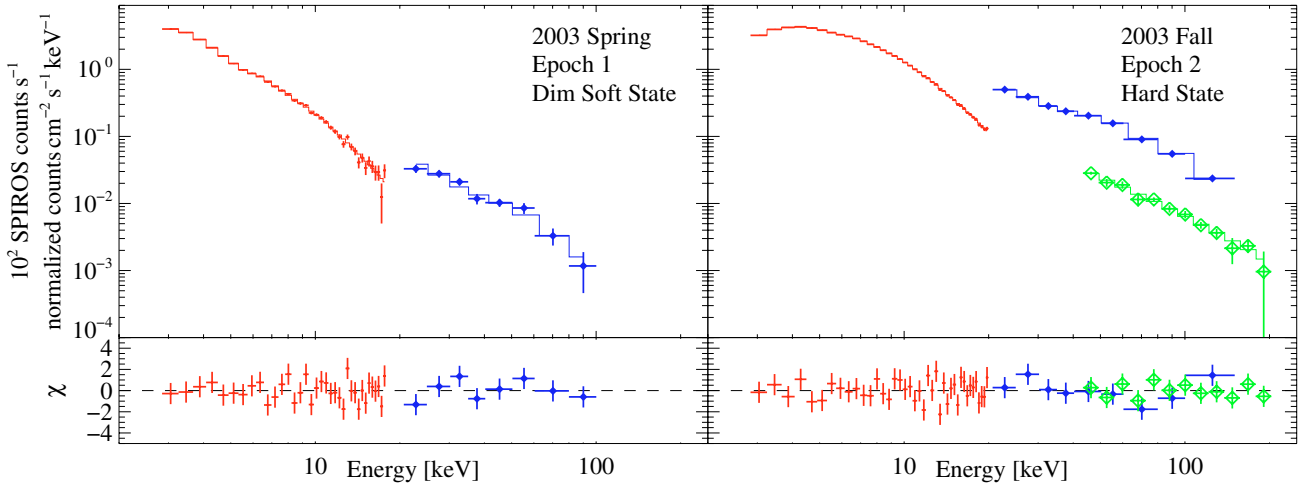

Fig. 3. Summed counts spectra for the GRS 1758−258 monitoring observations of 2003 spring (epoch 1) and 2003 fall (epoch 2) with the best fit `compTT` model and the corresponding residuals. Small dots are PCA, filled diamonds ISGRI, and open diamonds SPI data. For reasons of clarity only the first of the two SPI spectra for epoch 2 is shown but both data sets have been used to derive the plotted model and residuals as well as the best fit parameters listed in Tables 3 and 4. Note that "count rates" delivered by the SPI extraction software SPIROS are not directly comparable to those of other instruments and that here and in Fig. 4 the SPI spectra have additionally been multiplied by a factor of 100 for display purposes.

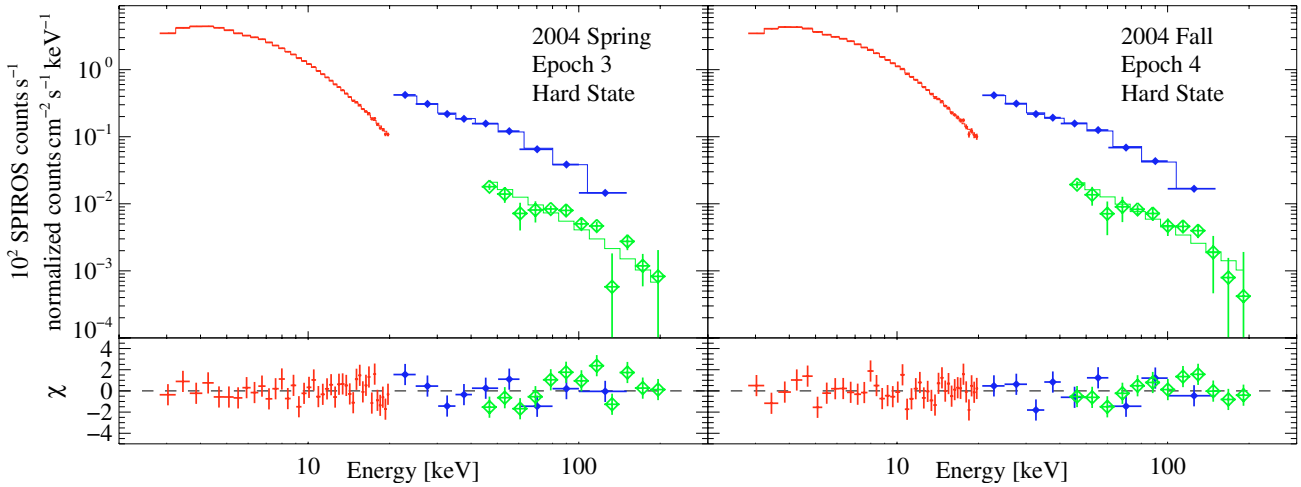

Fig. 4. The same as Fig. 3 but for the observations of 2004 spring (epoch 3) and 2004 fall (epoch 4).

INTEGRAL/*RXTE* spectra (Pottschmidt et al. 2003, 2004). While the `compTT`/`eqpair` discrepancy is likely due to the omission of relativistic smearing of the reflection spectrum in `compTT`, as recently suggested by Wilms et al. (2006) on the basis of `compTT` and `eqpair` fits to several hundred *RXTE* monitoring observations of Cyg X-1, this is not the case here since our `compPS` fits do not include relativistic smearing.

3.2.2. The 3−200 keV spectrum

As a Galactic Center source, GRS 1758−258 is known to be strongly absorbed and the $N_{\rm H}$ value adopted in most studies is $(1.5 \pm 0.1) \times 10^{22}$ cm^{-2}, as derived by Mereghetti et al. (1997) from *ASCA* observations. However, Keck et al. (2001) report $(0.98 \pm 0.08) \times 10^{22}$ cm^{-2} from *ROSAT* observations, Lin et al. (2000) find $(0.93{-}2.0) \times 10^{22}$ cm^{-2} from *RXTE* observations, and Goldwurm et al. (2001) determine $(1.74 \pm 0.07) \times 10^{22}$ cm^{-2} with *XMM*. Modeling PCA data starting at 3 keV, $N_{\rm H}$ and the blackbody parameters are known to be strongly correlated and not well constrained. Here, we obtain best fits with $N_{\rm H}$ values generally well consistent with the canonical value of 1.5×10^{22} cm^{-2} for epochs 1 and 2 (for the epoch 2 `cutoffpl` fit, though, $N_{\rm H}$ is closer to the lower value of Keck et al. 2001). In the case of epoch 1 this includes a `diskbb` component which is obviously required, while in the case of epoch 2 no thermal component is needed. For epochs 3 and 4 the best fits with free $N_{\rm H}$ result in too low values of $(0.03{-}0.7) \times 10^{22}$ cm^{-2} and freezing $N_{\rm H}$ to the canonical value does not produce acceptable fits. Adding a disk blackbody component, however, allows for good fits with the canonical $N_{\rm H}$ (frozen with exception of the epoch 4 `cutoffpl` fit). For the Comptonization fit of epoch 4 this procedure results in a somewhat higher plasma temperature and lower optical depth compared to the other hard state observations than without including the disk component (Table 4). The same tendency in presence of a disk blackbody is seen when holding $N_{\rm H}$ at the lower value of Keck et al. (2001). For all Comptonization fits the blackbody temperature has been tied to the seed photon temperature of the `compTT` component.

Clear residuals in the 6−7 keV range are present for all epochs when no iron line is included. The χ^2 values obtained when removing the Gaussian iron line from the models is given for reference in Table 3. Note that the F-test may not be used

to test for the presence of a line (Protassov et al. 2002). In epoch 4 the improvement of the fit when including the iron line is considerably smaller than for the other epochs and an acceptable fit can be achieved without the line ($\chi^2_{\rm red} = 1.09$), residuals remain, however. The iron line is generally narrow, with widths around or below 0.4 keV, and consistent with zero. The line energy ranges from 6.40 to 6.73 keV and is mostly consistent with 6.4 keV, i.e., neutral Fe. Interestingly, the one exception is epoch 3 where we also measure the strongest reflection component. A 3−4 times higher line equivalent width is measured for the soft state epoch 1, consistent with earlier measurements (Heindl & Smith 1998; Smith et al. 2001a; Sidoli & Mereghetti 2002). This mainly reflects the reduced level of continuum emission during that time, since the line normalization does not change significantly between the epochs, including the soft state. It has to be kept in mind, though, that the Galactic diffuse emission features a strong iron line and that the iron line parameters obtained from the fits are most likely influenced by a non-perfect correction for this emission.

The parameters we are mainly interested in are those characterizing the broad band continuum. We caution again that calibration uncertainties prohibit a statistical comparison with earlier results. Nevertheless we list earlier results for a qualitative comparison and to illustrate the overall picture. For epochs 2 to 4 we find values typical for hard state BHC spectra. For the phenomenological model the power law indices lie between $1.54^{+0.01}_{-0.02}$ (epoch 2) and $1.69^{+0.05}_{-0.05}$ (epoch 4) and the cutoff energies range from 136^{+13}_{-16} keV (epoch 3) to 246^{+26}_{-56} keV (epoch 4). Lin et al. (2000) find $\Gamma \sim 1.40$ (uncertainty of the order of 0.04) and $E_{\rm cutoff} \sim 200$ keV (uncertainty of the order of 30 keV) for their joint *RXTE* and *CGRO*/OSSE spectrum of 1997 and Kuznetsov et al. (1999) find $\Gamma = 1.0 \pm 0.3$ and $E_{\rm cutoff} = 89^{+40}_{-20}$ keV for their combined 1990−1997 *GRANAT* data (no cutoff was fit to shorter data sets). With 246 keV the cutoff energy for epoch 4 is at the limit of what can be measured with these observations. However, no good fit can be obtained without cutoff ($\chi^2_{\rm red} = 2.9$).

From the Comptonization models we obtain plasma temperatures of 78^{+34}_{-15} keV and 49^{+29}_{-9} keV and optical depths of $0.71^{+0.16}_{-0.07}$ and $1.00^{+0.21}_{-0.21}$ for epochs 2 and 3. Here the values of Lin et al. (2000) are $kT_{\rm e} \sim 52$ keV (uncertainty of the order of 7 keV) and $\tau \sim 3.4$ (uncertainty of the order of 0.3). Similarly, Sidoli & Mereghetti (2002) find values of $kT_{\rm e} = 44^{+146}_{-7}$ keV and $\tau = 3.6^{+0.4}_{-2.3}$ for their *BeppoSAX* data set. In both of these cases the higher optical depth is probably mainly due to two effects, first the fact that no reflection component has been included in the models and second that the sphere+disk geometry has been used. We see a moderate trend towards higher values of τ when switching from slab to sphere+disk geometry in our fits.

Kuznetsov et al. (1999) obtain $kT_{\rm e} = 41^{+7}_{-5}$ keV and $\tau = 1.2 \pm 0.2$. However, they were using a predecessor to `compTT`, namely the model of Sunyaev & Titarchuk (1980), therefore their results cannot be directly compared to ours. Also, these values reflect the average over a wide range of $kT_{\rm e}$ and τ values obtained from their two observation periods each year.

In the Comptonization fits we also allow for reflection of the Comptonized radiation of a cold accretion disk and find reflection factors of $10.0^{+5.6}_{-5.6}$% and $13.8^{+5.0}_{-5.5}$% for epochs 2 and 3, respectively. No reflection is detected in epoch 4. From the `cutoffpl` fits it is also clear that the epoch 4 spectrum is less curved than the other two hard state spectra. With $kT_{\rm e} = 114^{+32}_{-35}$ keV and $\tau = 0.37^{+0.24}_{-0.12}$ the Comptonization parameters of epoch 4 correspond to the hottest and most transparent plasma among the hard state observations. While the latter might be an artifact due to the introduction of the disk blackbody necessary to constrain $N_{\rm H}$ (the Compton-y changes only slightly)[4], a possible physical origin for the differences observed in the epoch 4 spectrum is suggested by the occurrence of one of the sudden moderate drops in the PCA rate during this time (see Fig. 2 and Sect. 3.1).

In general, the range of different results for the hard state parameters is not too surprising in the light of the considerable long term variations known to be present even within the hard state (Fig. 2), however, it is also clear that *INTEGRAL* calibration caveats apply. With $kT_{\rm e} \sim 50$−60 keV, $\tau \sim 1.0$−1.2, and reflection fractions of 17−24% the `compTT` fits of Pottschmidt et al. (2003) to a set of *INTEGRAL* and *RXTE* observations of Cyg X-1 result in similar parameters as observed for epoch 3.

As expected from the long term evolution of the light curves, the spectrum of epoch 1 differs considerably from the others. In both models an additional soft component of comparable strength is clearly present. We obtain a multicolor disk blackbody temperature of 477^{+11}_{-27} eV from the power law fit and of 482^{+14}_{-16} eV from the Comptonization fit. This is consistent with the 2001 dim soft state where Smith et al. (2001a) found a disk blackbody temperature of 464 ± 7 eV with the PCA, Miller et al. (2002) give values of 340 ± 10 eV and 600 ± 10 eV, depending on $N_{\rm H}$, for *XMM* observations, and Heindl & Smith (2002b) find 505 ± 7 eV with *Chandra*. Based on these previously measured soft state values and since the soft state spectrum is dominated by disk emission below ∼5 keV, we believe that the values quoted above give a realistic measure of the temperature. Not surprisingly the seed photon/disk temperature is not well constrained in the hard state observations. For epoch 3, e.g., the disk temperatures obtained from the cutoff power law and the Comptonization fits are formally not consistent but what is consistent is the fact that in both cases the disk component is needed if $N_{\rm H}$ is assumed to lie within the range of previously measured values. Where a disk blackbody component was included in the hard state fits it never dominates the soft spectrum. With $\Gamma = 2.29^{+0.10}_{-0.05}$ the power law is significantly steeper in epoch 1 but does not quite reach the value of $\Gamma = 2.75 \pm 0.12$ observed in 2001 March (Smith et al. 2001a). No cutoff is detected but during this time the high energy flux was comparatively weak and the spectrum could only be obtained out to 100 keV. The steepness of the spectrum translates into a small optical depth of $0.29^{+0.43}_{-0.13}$ in the Comptonization fit, while the temperature of the hot plasma is found to be 64^{+4}_{-15} keV, i.e., not significantly different from the hard state epochs 2 and 3.

4. Discussion

Is the dim soft state of GRS 1758−258 really that different from the soft states observed in other sources? In Fig. 5 the unfolded, unabsorbed model spectra corresponding to the `compTT` fits are shown. The typical pivoting between the soft state spectrum and the three hard state spectra is seen. With ∼3 keV the pivot energy lies considerably lower than for Cyg X-1, where a value of about ∼10 keV is observed (Zdziarski et al. 2002; Wilms et al. 2006). However, taking the nature of GRS 1758−258 as low mass X-ray binary (LMXB) and Roche lobe accretor into account, its behavior might be more akin to the state transitions displayed by

[4] Note, however, that apart from the already quoted effect of obtaining a higher reflection fraction, the best fit parameters obtained with `compPS` for epoch 4 show the same tendency ($kT_{\rm in} = 521$ eV, $kT_{\rm e} = 102$ keV, $\tau = 0.63$, $\Omega/2\pi = 0.05$, and $\chi^2_{\rm red} = 0.95$) although no additional disk blackbody has been included.

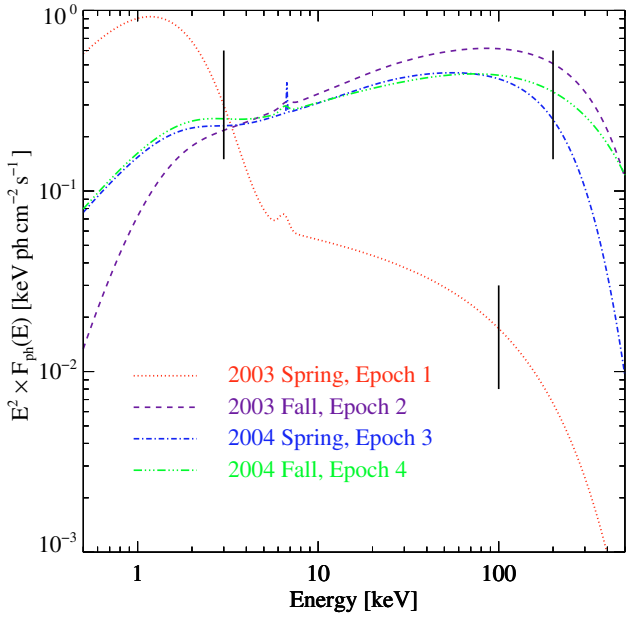

Fig. 5. Unfolded, unabsorbed model spectra corresponding to the `compTT` fits listed in Table 4. The N_H values quoted in that table have been used for the flux correction. Vertical lines denote the range of the modeled data.

LMXB BHC transients than to those of the high mass X-ray binary (HMXB) and focused wind accretor Cyg X-1, i.e., hysteresis might play an important role. In the following the term "hysteresis" is used to describe the existence of an "overlap region" in luminosity in which both, soft and hard states can occur (see, e.g., Miyamoto et al. 1995; Zdziarski & Gierliński 2004; Meyer-Hofmeister et al. 2005)[5]. According to the rough estimate for the bolometric luminosity that can be derived from our fits (using a distance estimate of 8.5 kpc based on the assumption of a near-GC location of GRS 1758−258), the 2003 dim soft state is 0−20% less luminous than the hard state, depending on the hard state epoch and spectral model used for comparison. For a 10 $M_\odot$ black hole the hard state luminosities that we measure correspond to 2−3% $L_{\rm Edd}$. The differences between the states in terms of fluxes in different energy bands have been presented in Table 2.

Before comparing the range of hysteretic behavior observed in GRS 1758−258 to other sources, we note that another possible reason for observing reduced soft state luminosities might be a geometric effect introduced by the inclination i of the system: In the hard state the geometrically thick hot plasma is present which can be assumed to radiate approximately isotropically. In the soft state only the decaying accretion disk remains which is geometrically thin with a luminosity $\propto \cos i$ (Frank et al. 1992). If the system is viewed close to edge-on the projected area of the inner disk is comparatively small, allowing only for a small percentage of the disk luminosity to reach the observer. In addition, X-rays from the inner disk may be further obscured due to flaring of the outer disk (Narayan & McClintock 2005).

GX 339−4 is the source for which hysteresis in the above sense has been best studied so far. Depending on the energy range, its lowest soft state flux can lie a factor of 2.5−10 below the brightest hard state flux (Nowak et al. 2002; Zdziarski et al. 2004; Belloni et al. 2005). Nowak et al. (2002), e.g., find that the 3−9 keV soft state flux can be less than half the hard state flux, similar to what we find for GRS 1758−258 (Table 2). The bolometric flux of GX 339−4 in the soft state can be up to an order of magnitude lower than in the hard state (Zdziarski et al. 2004), an even more extreme behavior than indicated by our bolometric estimates for GRS 1758−258. Accordingly, the schematic picture which has recently been developed of the "q-shaped" tracks followed by black hole transients in the hardness-intensity diagram over an outburst includes a large range of soft state intensities ($\gtrsim O(1)$, Fender et al. 2004), not necessarily exceeding the highest hard state ones. Although we concentrate on average soft state parameters in this work, we want to note that the hardness-intensity diagrams for the 2003 soft state that can be derived from the energy-resolved PCA light curves show a counterclockwise evolving pattern comparable to transients. Due to the pronounced soft state it is rather slightly "p-shaped" but otherwise qualitatively very similar (a detailed quantitative comparison is beyond the scope of this work). Overall it seems that GRS 1758−258's dim soft state of 2003 – and also the even dimmer one of 2001 – are no remarkable states for a non high mass BHC (see also Remillard 2005). This is especially true if part of the luminosity reduction in the dim soft state is due to the inclination effect described above. How about the overall state evolution, though? Can the occurrence of the dim soft states be understood in the frame of the outburst evolution scheme mentioned above? In the following two paragraphs we discuss this question on the basis of the light curves displayed in Figs. 1 and 2. Note, however, that a detailed spectral analysis of the individual PCA pointings is beyond the scope of this paper.

The initial phase of the state change consists of a sudden drop of the >4 keV count rate around JD 2 452 680 (2003 February) and a simultaneous moderate brightening of the thermal component, observed as a ∼70% increase in the 2.5−4 keV count rate. Only two monitoring observations find the source in this phase, i.e., it lasted roughly a week. During the following weeks the dim soft state is observed: the hard emission does not recover until end of 2003 April and after the initial increase the soft emission decays slowly to a low hard state level. The initial outburst-like phase is similar to a canonical transition to a soft state but with the system not settling into a state with a stable thermal component. In this sense the episode is a "failed state transition". The short soft flare may reflect an actual change in the accretion disk parameters (e.g., a temperature change and/or a change of the inner disk radius). Alternatively, the increase in soft photon flux could at least partly be caused by the disappearance of the Comptonizing medium, i.e., the soft photons acting as seed photons in the hard state are now emerging without being Comptonized. While the 2001 dim soft state showed no initial flaring of the 2.5−4 keV count rate, a soft excess compared to the hard state level also became visible in the unabsorbed spectrum.

In contrast to the weeks long soft X-ray flares of Cyg X-1, however, for which the term "failed state transition" was coined (Pottschmidt et al. 2000, 2003), GRS 1758−258 does not settle back into the hard state after the flaring but the hard component stays "off". In the case of the 2001 dim soft state Smith et al. (2001a) suggested a sudden shutoff of mass transfer from the companion being responsible for the "off" phase. Put into the context of the "q" pattern of transient outbursts, the dim soft states of GRS 1758−258 could therefore well represent the thermally dominated outburst phase since the main decay track proceeds through this state (Remillard 2005). The hard state of GRS 1758−258, also covering a considerable range of luminosities, would then correspond to phases of rising and peak

[5] The flux derivative/hardness correlation may represent the extension of this hysteretic behavior into the hard state (Smith et al. 2002b).

luminosities, again consistent with transient outbursts. As mentioned in Sect. 1, additional intermediate states – or failed state transitions – of GRS 1758−258 have been observed (Mereghetti et al. 1994; Goldwurm et al. 2001; Heindl & Smith 2002a), further completing the outburst picture.

Another interesting property of the dim soft state is the fact that the decay of the hard and soft spectral components is governed by two different time scales. This has been studied in detail for the 2001 dim soft state by Smith et al. (2001a) who found that while the power law flux decreased by an order of magnitude from one monitoring observation to the next, the disk black body flux decayed on a time scale of ∼28 d. This behavior is also visible in the 2003 light curves (Fig. 1), especially in the fast decline of the 10−25 keV rates and the much slower trend in the 2.5−4 keV rates after the initial drop down from the "failed state transition" level. The source also shows several drops of the hard component for durations of only a few days or less, e.g., around JD 2 451 932 (2001 January, see Fig. 2 and Smith et al. 2001a), 2 452 364 (2002 March, Fig. 2), 2 452 788 (2003 May, Fig. 1), or 2 452 855 (2003 August, Fig. 1). All these quasi-independent changes of the hard and soft spectral component further support the interpretation of the behavior of GRS 1758−258 in terms of two different accretion flows. As shown by Smith et al. (2001a), the model of Chakrabarti & Titarchuk (1995) can explain many of the observations. As already mentioned, this model assumes that proportional accretion rate changes introduced to both flows at large radii propagate with nearly the free-fall time scale through the Comptonizing medium and independently on the viscous time scale through the accretion disk. Different propagation speeds are a general feature of the model, i.e., they are not restricted to its high accretion rate soft state associated with bulk motion Comptonization. For lower accretion rates complicated dependencies of spectral hardness and accretion rate are possible, covering the correlation between the flux derivative and the spectral hardness as well as the dim soft state (Chakrabarti & Titarchuk 1995; Smith et al. 2001a). The strength of these time delay effects increases for larger accretion disks and there are indications that such a picture might be generally applicable for Roche lobe overflow transients: a state transition due to a sudden change in the power law component during a time when the disk black body parameters evolved smoothly has recently also been seen in the black hole transient H1743−322, in this case marking the transition between the thermally dominant and the intermediate state (Kalemci et al. 2006).

In addition to soft episodes we also observe several occurrences of a rather sudden hardening (Fig. 6) mainly due to declines of the soft component, visible, e.g., in the 2.5−4 keV rates around JD 2 452 797 (2003 June), 2 453 148 (2004 May), or 2 453 261 (2004 September). In the first case this is clearly related to a preceding drop of the hard component. In the second case the drop happens at the end of a months long decline of the count rates in all energy bands which is especially visible in the *INTEGRAL* range (epoch 3). The situation is less clear for the third occurrence (during epoch 4) but the 10−25 keV light curve also indicates a preceding decline. Due to this overall picture and the probably affected broad band spectrum of epoch 4, we consider it less likely that the hard episodes are caused, e.g., by absorption events, but are rather another example of the quasi-independent behavior of the hard and soft component on different time scales. Interestingly, a similar episode of sudden hardening has also been observed for the "two-flow source" 1E 1740.7−2942 (Smith et al. 2002b).

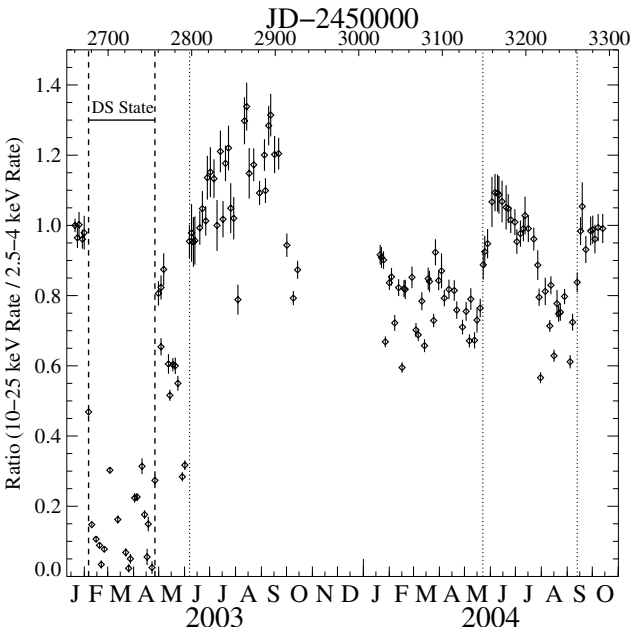

Fig. 6. Ratio of the 10−25 keV and 2.5−4 keV PCA count rates. Dashed and dotted vertical lines denote the dim soft state of 2003 and times of sudden hardening, respectively.

Finally, while the hard state parameters have been discussed in Sect. 3.2.2 already, we emphasize again that apart from small peculiarities which might be caused by spectral variations within the epochs (epoch 4) the epoch-summed hard state spectra can be well described by cutoff power law and thermal Comptonization parameters which are compatible with canonical values found for BHCs in the hard state, e.g., Cyg X-1.

5. Summary

We have presented analyses of *INTEGRAL* and *RXTE* monitoring observations of the Galactic Center BHC GRS 1758−258 obtained in 2003 and 2004. Energy-resolved light curves from 2.5 to 200 keV have been studied and broad band spectra accumulated over four ∼2−3 months long *INTEGRAL* observing epochs have been modeled phenomenologically and with thermal Comptonization. The main results of this work can be summarized as follows:

- From 2003 February to April GRS 1758−258 entered another dim soft state (partly covered by epoch 1) similar to but less prolonged than the one observed in 2001.
- Phenomenological models (dominated by a power law in the dim soft state and an exponentially cutoff power law in the hard states) as well as thermal Comptonization models (`compTT` and `compPS`) allow for a good description of the epoch-summed spectra.
- The fit parameters obtained in the hard state are canonical BHC hard state parameters, similar to those obtained for Cyg X-1 and generally consistent with previous results obtained for GRS 1758−258. The hard state in GRS 1758−258 is known to be intrinsically variable. Since it is not clear how much of the range of the fit parameters observed between the hard state epochs is due to calibration uncertainties, however, these differences are not interpreted further.
- In the dim soft state the flux is only higher than in the hard state below 3−4 keV. In all other energy bands the flux is considerably lower. A tentative estimate of the bolometric

luminosity, however, shows a reduction of only 0−20% compared to the hard state epochs.
- While the dim soft state is different from the soft state in persistent HMXBs like Cyg X-1 or LMC X-3 where softening is associated with higher luminosities (mass accretion rates), it is well within the range of hysteretic behavior displayed by LMXB transients like GX 339−4, where a large range of soft state intensities, not necessarily exceeding the highest hard state ones, is observed ("q" pattern in the hardness-intensity diagram). The dim soft state would thus correspond to the outburst decay of a transient. This can be understood since GRS 1758−258 most likely has a low mass companion and is accreting via Roche lobe overflow.
- As discovered for the 2001 dim soft state by Smith et al. (2001a), the decay of the soft and hard component progresses on different time scales which can be understood if the accretion flows through the cool disk and the hot plasma are independent in the sense of the two-flow model of Chakrabarti & Titarchuk (1995). The evolution of the light curves, especially comparing the 2.5−4 keV and 10−25 keV PCA bands during the 2003 dim soft state also suggests different time scales for changes in the two spectral components.
- In addition, several instances are observed during which predominantly one of the two spectral components shows a substantial flux change from one monitoring observation to the next, further supporting the picture of at least partly independent flows.

Acknowledgements. We thank Jörn Wilms for helpful discussions. This work has been partly funded by NASA contract NAS5-30720 (KP) as well as by NASA grants NAG5-13576 and NNG04GP41G (DMS, NB). AAZ and PL have been supported by KBN grants 1P03D01827, 1P03D01727, 1P03D01128, PBZ-KBN-054/P03/2001 and 4T12E04727. This work is based on observations with *INTEGRAL*, an ESA project with instruments and science data centre funded by ESA member states (especially the PI countries: Denmark, France, Germany, Italy, Switzerland, Spain), Czech Republic and Poland, and with the participation of Russia and the USA. We thank the *RXTE* schedulers for making the years long monitoring campaign of GRS 1758−258 possible. KP thanks the Aspen Center for Physics for its hospitality during the final stages of the preparation of this paper.

References

Belloni, T., Homan, J., Casella, P., et al. 2005, A&A, 440, 207
Chakrabarti, S., & Titarchuk, L. G. 1995, ApJ, 455, 623
Coppi, P. S. 1999, in High Energy Processes in Accreting Black Holes, ed. J. Poutanen, & R. Svensson (San Francisco: ASP), ASP Conf. Ser., 161, 375
Dubath, P., Knödlseder, J., Skinner, G. K., et al. 2005, MNRAS, 357, 420
Eikenberry, S. S., Fischer, W. J., Egami, E., & Djorgovski, S. G. 2001, ApJ, 556, 1
Fender, R. P., Belloni, T. M., & Gallo, E. 2004, MNRAS, 355, 1105
Frank, J., King, A., & Raine, D. 1992, Accretion Power in Astrophysics (Cambridge: Univ. Cambridge Press)
Gilfanov, M., Churazov, E., Sunyaev, R., et al. 1993, ApJ, 418, 844
Goldwurm, A., David, P., Foschini, L., et al. 2003, A&A, 411, L223
Goldwurm, A., Israel, D., Goldoni, P., et al. 2001, in Proc. of the Gamma-Ray Astrophysics 2001 Symposium (Woodbury: AIP), AIP Conf. Proc., 587, 61
Grebenev, S. A., Pavlinsky, M. N., & Sunyaev, R. A. 1997, in The Transparent Universe, ed. C. Winkler, T. J. L. Courvoisier & P. Durouchoux (Noordwijk: ESA Publications Division), ESA SP, 382, 183
Heindl, W. A., & Smith, D. M. 1998, ApJ, 506, L35
Heindl, W. A., & Smith, D. M. 2002a, ApJ, 578, L125
Heindl, W. A., & Smith, D. M. 2002b, in The High Energy Universe at Sharp Focus: Chandra Science, ed. E. M. Schlegel, & S. D. Vrtilek (San Francisco: ASP), ASP Conf. Ser., 262, 241
Jahoda, K., Swank, J. H., Giles, A. B., et al. 1996, in EUV, X-Ray, and Gamma-Ray Instrumentation for Astronomy VII, ed. O. H. Siegmund (Bellingham, WA: SPIE), Proc. SPIE, 2808, 59
Kalemci, E., Tomsick, J. A., Rothschild, R. E., et al. 2006, ApJ, 639, 340
Keck, J. W., Craig, W. W., Hailey, C. J., et al. 2001, ApJ, 563, 301
Kuznetsov, S. I., Gilfanov, M. R., Churazov, E. M., et al. 1999, Astron. Lett., 25, 351
Lebrun, F., Leray, J. P., Lavocat, P., et al. 2003, A&A, 411, L141
Lin, D., Smith, I. A., Liang, E. P., et al. 2000, ApJ, 532, 548
Lund, N., Budtz-Jørgensen, C., Westergaard, N. J., et al. 2003, A&A, 411, L231
Magdziarz, P., & Zdziarski, A. A. 1995, MNRAS, 273, 837
Main, D. S., Smith, D. M., Heindl, W. A., et al. 1999, ApJ, 525, 901
Mandrou, P. 1990, IAU Circ., 5032
Marti, J., Mereghetti, S., Chaty, S., et al. 1998, A&A, 338, L95
Mereghetti, S., Belloni, T., & Goldwurm, A. 1994, ApJ, 433, L21
Mereghetti, S., Cremonesi, D. I., Haardt, F., et al. 1997, ApJ, 476, 829
Meyer-Hofmeister, E., Liu, B. F., & Meyer, F. 2005, A&A, 432, 181
Miller, J. M., Wijnands, R., Rodriguez-Pascual, P. M., et al. 2002, ApJ, 566, 358
Miyamoto, S., Kitamoto, S., Hayashida, K., & Egoshi, W. 1995, ApJ, 442, L13
Narayan, R., & McClintock, J. E. 2005, ApJ, 623, 1017
Nowak, M. A., Wilms, J., & Dove, J. B. 2002, MNRAS, 332, 856
Pottschmidt, K., Wilms, J., Nowak, M. A., et al. 2000, A&A, 357, L17
Pottschmidt, K., Wilms, J., Chernyakova, M., et al. 2003, A&A, 411, L383
Pottschmidt, K., Wilms, J., Nowak, M. A., et al. 2004, in Proc. 5th INTEGRAL Workshop: The INTEGRAL Universe, ed. V. Schönfelder, G. Lichti, & C. Winkler (Noordwijk: ESA), ESA SP-552, 345
Poutanen, J., & Svensson, R. 1996, ApJ, 470, 249
Protassov, R., van Dyk, D. A., Connors, A., et al. 2002, ApJ, 571, 545
Remillard, R. A. 2005, in Texas@Stanford 2004, ed. P. Chen, SLAC Electronic Conference Proceedings Archive [arXiv:astro-ph/0504129]
Rodriguez, L. F., Mirabel, I. F., & Marti, J. 1992, ApJ, 401, L15
Rothstein, D. M., Eikenberry, S. S., Chatterjee, S., et al. 2002, ApJ, 580, L61
Sidoli, L., & Mereghetti, S. 2002, A&A, 388, 293
Skinner, G., & Connell, P. 2003, A&A, 411, L123
Smith, D. M., Heindl, W. A., Swank, J., et al. 1997, ApJ, 489, L51
Smith, D. M., Heindl, W. A., Markwardt, C. B., & Swank, J. H. 2001a, ApJ, 554, L41
Smith, D. M., Heindl, W. A., Swank, J. H., & Markwardt, C. B. 2001b, ATEL, 66
Smith, D. M., Heindl, W. A., & Swank, J. H. 2002a, ApJ, 578, L129
Smith, D. M., Heindl, W. A., & Swank, J. H. 2002b, ApJ, 569, 362
Strong, A. W., Bouchet, L., Diehl, R., et al. 2003, A&A, 411, L447
Sunyaev, R., Churazov, E., Gilfanov, M., et al. 1991, A&A, 247, L29
Sunyaev, R. A., & Titarchuk, L. G. 1980, A&A, 86, 121
Terrier, R., Lebrun, F., Bazzano, A., et al. 2003, A&A, 411, L167
Titarchuk, L. 1994, ApJ, 434, 570
Vedrenne, G., Roques, J. P., Schönfelder, V., et al. 2003, A&A, 411, L63
Wilms, J., Nowak, M. N., Pottschmidt, K., et al. 2006, A&A, 447, 245
Zdziarski, A. A., & Gierliński, M. 2004, Progress Theor. Phys. Suppl., 155, 99
Zdziarski, A. A., Poutanen, J., Paciesas, W. S., & Wen, L. 2002, ApJ, 578, 357
Zdziarski, A. A., Gierliński, M., Mikołajewska, J., et al. 2004, MNRAS, 351, 791
Zhang, S. N., Cui, W., Harmon, B. A., et al. 1997, ApJ, 477, L95